



Hydrogen absorption and ^{57}Fe Mössbauer effect in UFeGe

A.M. Adamska^{a,b,*}, L. Havela^a, A. Błachowski^c, K. Ruebenbauer^c,
J.C. Waerenborgh^d, Nhu-T.H. Kim-Ngan^{a,e}, A.V. Kolomiets^{a,f}

^a Department of Condensed Matter Physics, Faculty of Mathematics and Physics, Charles University, Ke Karlovu 5, 12116 Prague 2, Czech Republic

^b Faculty of Physics and Applied Computer Science, AGH University of Science and Technology, al. Mickiewicza 30, PL-30 059 Kraków, Poland

^c Mössbauer Spectroscopy Division, Institute of Physics, Pedagogical University, ul. Podchorążych 2, PL-30-084 Kraków, Poland

^d Instituto Tecnológico e Nuclear/CFMC-UL, Química, 2686-953 Sacavém, Portugal

^e Surface Physics Division, Institute of Physics, Pedagogical University, ul. Podchorążych 2, PL-30-084 Kraków, Poland

^f Department of Physics, National University "Lvivska Polytechnika", Bandery 12, 79013 Lviv, Ukraine

ARTICLE INFO

Article history:

Received 6 January 2011

Received in revised form 14 February 2011

Accepted 16 February 2011

Available online 23 February 2011

Keywords:

Hydrides

Crystal structure

Actinides

Mössbauer spectroscopy

ABSTRACT

Hydrogenation of UFeGe transforms the monoclinic type of structure into the orthorhombic (TiNiSi-type) and subsequently to the hexagonal (ZrBeSi-type) structure. It does not induce magnetic order, however magnetic susceptibility is enhanced. The Sommerfeld coefficient γ increases from 12 mJ/mol K² in UFeGe to 36 mJ/mol K² in UFeGeH_{1.7–1.8} (β -hydride). The observed variations of electronic properties are mainly due to the modified geometry of the lattice, characterized by enhanced inter-uranium spacing, and reduced 5f–3d hybridization in the hydrides.

© 2011 Elsevier B.V. All rights reserved.

1. Introduction

UFeGe belongs to a large UTGe family. Unlike e.g. the unconventional ferromagnetic superconductor UCoGe with the common TiNiSi-type of structure, it undergoes a monoclinic distortion (low-temperature LT phase) (space group $P2_1/m$). The monoclinic distortion is removed above 500 K, where a structural transition to the orthorhombic TiNiSi-type (high-temperature HT phase) is observed [1]. Due to rather strong 5f–3d hybridization ($d_{\text{U2-Fe2}} = 3.360 \text{ \AA}$, the compound is expected to be non-magnetic, nevertheless the electrical resistivity measurement had led to a speculation about magnetic ordering below 80 K associated with a broad maximum around this temperature [1]. A maximum was also detected in dc susceptibility and interpreted as a consequence of spin fluctuations, χ reaches only about $3 \times 10^{-8} \text{ m}^3/\text{mol}$ [2]. Magnetism of U compounds can be to some extent stimulated by hydrogenation and concomitant volume expansion. An increase of inter-uranium distances may allow a magnetic order of U lattice provided weaker 5f-ligand hybridisation, which could lead to a long-range magnetic order. The effect of hydrogenation is

already known for other members of the UTGe family, i.e. two weak itinerant ferromagnets URhGe [3,4] and UCoGe [5]. In the first case, the highest applied pressure of H₂ gas was not sufficient to change the type of structure, an α -hydride (a solid solution of small amount of hydrogen randomly distributed in the lattice) of URhGe with less than 0.1 H/f.u. crystallizes in the TiNiSi-type of structure expanded by about 1%. Despite such low expansion, hydrogenation has significant impact on magnetic properties of URhGe, namely its Curie temperature is enhanced in the hydride, and reaches about 20 K. Another type of behaviour was reported for UCoGe. Relatively low hydrogen pressure of 5 bar allows to reach a high H content of 1.7 H/f.u., and transforms the crystal structure from the orthorhombic TiNiSi-type to hexagonal one (ZrBeSi-type), with approximately 10% volume expansion. The β -hydride (H-rich phase significantly expanded, adopting usually different type of structure than the pure compound) exhibits a ferromagnetic transition in the vicinity of 50 K. Also an α -hydride of UCoGe (0.1 H/f.u.) was synthesised at low hydrogen pressure of 2 bar. Its crystal structure remains orthorhombic as in the parent compound, and expands by about 0.25%. Surprisingly the weak ferromagnetism observed in the precursor sample of UCoGe, is entirely lost in the α -hydride [5]. Keeping in mind such pronounced and non-trivial effects of hydrogenation on the magnetism in UTGe system, we found it particularly interesting to investigate how the weak paramagnetism of UFeGe would react to the H insertion.

* Corresponding author at: Department of Condensed Matter Physics, Faculty of Mathematics and Physics, Charles University, Ke Karlovu 5, 12116 Prague 2, Czech Republic. Tel.: +420 22191 1351; fax: +420 22191 1351.

E-mail address: anna@mag.mff.cuni.cz (A.M. Adamska).

2. Experimental details

A polycrystalline sample of UFeGe was prepared by arc melting of stoichiometric amounts of the constituent metals. The crystal structure was investigated by means of XRD–3003 Seifert diffractometer (Cu K α radiation). For the hydride synthesis, bulk material crushed into sub-millimeter particles was placed into a reactor. The typical hydrogenation process consists of three steps. At first, the sample is activated by heating up to $T=523\text{ K}$ under high-vacuum conditions (pressure of 10^{-6} mbar), subsequently the activated material is exposed to pure hydrogen gas. Depending on its pressure, various H stoichiometries can be achieved. Last step is thermal cycling of the sample up to $T=773\text{ K}$ at a given H pressure to promote the hydrogen absorption. In the course of present study, two hydrogenation attempts of UFeGe were made. The first one resulted in pure β -hydride obtained under the highest possible H_2 pressure of 156 bar. During the second attempt, the hydrogen pressure of 2 bar and thermal cycling up to 723 K was applied, yielding an α -hydride of UFeGe. In the previous test, with the intermediated hydrogen pressure of 96 bar, a mixed α - and β -hydride was obtained [3]. The main indication of the H absorption is a variation of crystal structure parameters indicated by X-ray powder diffraction (XRD). The absolute amount of absorbed hydrogen was determined by thermally induced desorption into an evacuated calibrated volume. Magnetic properties were studied both for UFeGe and its hydrides by means of an extraction magnetometer in the Quantum Design Physical Properties Measuring System (PPMS) and SQUID magnetometers in applied external fields up to 9 T and 7 T, respectively. The samples were in the form of randomly oriented powder fixed by a glue to avoid orientation of the grains by magnetic field and preferential orientation. Specific heat measurement was performed at the PPMS measuring system, using samples in the form of pellets compressed from the fine powder. Room temperature Mössbauer spectrum for UFeSi (for comparison) and room temperature spectrum for UFeGe were collected in transmission mode using a conventional constant-acceleration spectrometer and a 25 mCi ^{57}Co source in a Rh matrix; the velocity scale was calibrated using α -Fe foil. The spectra were fitted to Lorentzian lines using a non-linear least-squares method. UFeGe and its β -hydride spectra were collected using the MsAa-3 spectrometer with the commercial $^{57}\text{Co(Rh)}$ source kept at room temperature. The absorbers were prepared by mixing 40 mg/cm 2 of the samples with the B_4C carrier and then pressed into holders with both sides aluminised mylar windows. The low-temperature Mössbauer data were processed within transmission integral approximation as implemented in the MOSGRAF system.

3. Experimental results

3.1. Crystal structure

The crystal structure refinement of UFeGe provided the monoclinic crystal structure with room temperature lattice parameters $a=6.977(1)\text{ \AA}$, $b=4.305(1)\text{ \AA}$, $c=6.983(1)\text{ \AA}$, $\beta=93.7^\circ$ (space group $P2_1/m$). Atomic positions and coordinates are presented in Table 1. During the hydrogenation process under $p_{\text{H}_2}=96\text{ bar}$, 80% of the monoclinic phase was transformed into the hexagonal one (ZrBeSi-type), the rest remained as the high temperature phase of UFeGe (UFeGe $_{\text{HT}}$), an estimate of the hydrogen content gave a value 1.7 H/f.u. in average [3].

Table 2
Hydrogen pressure p_{H_2} , lattice parameters a , b and c , unit cell volume V , relative lattice expansion $\Delta a/a$, $\Delta b/b$ and $\Delta c/c$ along a -, b - and c -direction, respectively, in the representation of orthorhombic unit cell (the c lattice of UFeGe was recalculated for the orthorhombic representation: $c_{\text{orth}}=c_{\text{mon}}\cos(3.7^\circ)$), relative volume expansion $\Delta V/V$, the shortest $d_{\text{U-U}}$, $d_{\text{U-Fe}}$, $d_{\text{U-Ge/Si}}$ distances for UFeGe, UFeSi and their hydrides are given. Notice the change in notation between the two structure types: a_{orth} corresponds to c_{hex} , b_{orth} to d_{hex} and c_{orth} to $\sqrt{3}a_{\text{hex}}$.

Structure type	UFeGe Monoclinic ($\beta=93.7^\circ$)	UFeGeH $_{0.3}$ TiNiSi (orthorhombic)	UFeGeH $_{1.7-1.8}$ ZrBeSi (hexagonal)	UFeSi TiNiSi (orthorhombic)	UFeSiH $_{0.3}$ 70% of ZrBeSi (hexagonal)
p_{H_2} (bar)	–	2	156	–	140
a (Å)	6.977(1)	6.781(2)	4.176(1)	6.996(1)	4.044(1)
b (Å)	4.305(1)	4.182(1)	–	4.061(1)	–
c (Å)	6.983(1)	7.412(2)	7.337(2)	6.857(1)	7.787(1)
Volume per f.u. (Å 3)	52.33	52.55	55.42	48.70	55.15
($\Delta a/a$) $_{\text{orth}}$ (%)	–	–2.8	5.2	–	11.3
($\Delta b/b$) $_{\text{orth}}$ (%)	–	–3.0	–3.0	–	–0.4
($\Delta c/c$) $_{\text{orth}}$ (%)	–	6.3	3.8	–	2.1
$\Delta V/V$ (%)	–	0.5	6.0	–	13.0
$d_{\text{U-U}}$ (Å)	3.45	3.45	3.67	3.68	3.89
$d_{\text{U-Fe}}$ (Å)	2.35 ^a	2.95	3.00	3.00	3.00
$d_{\text{U-Ge/Si}}$ (Å)	2.97 ^b	2.91	3.00	2.90	3.00

^a The shortest distances between respective U2–Fe2 atoms.
^b The shortest distances between respective U1–Ge2 atoms.

Table 1
Atomic coordinates for UFeGe.

Atom	Position	x	y	z
U1	2e	0.0190(1)	0.25	0.7212(1)
U2	2e	0.5107(1)	0.25	0.8076(1)
Fe1	2e	0.3323(3)	0.25	0.4367(3)
Fe2	2e	0.7486(3)	0.25	0.0619(3)
Ge1	2e	0.2076(2)	0.25	0.1215(2)
Ge2	2e	0.7197(2)	0.25	0.3994(2)

An α -hydride of UFeGe with H content of 0.3 H/f.u. was successfully synthesised under $p_{\text{H}_2}=2\text{ bar}$ and thermal cycling only up to 723 K (in order to avoid the structure transformation during the hydrogenation process). The monoclinic symmetry was lifted to orthorhombic (TiNiSi-type), reaching 0.4% of volume expansion, which is clearly the effect of hydrogen absorption. The expanded orthorhombic structure is stable at room temperature. UFeGe $_{\text{HT}}$ is expanded by about 1.2% in respect to monoclinic phase, which means that the temperature effect is stronger than the effect of hydrogen absorption in this case.

After the previous study [3] the question remained if 20% of the orthorhombic phase in the hydride was UFeGe $_{\text{HT}}$ stabilized somehow to room temperature or an α -hydride of UFeGe. Closer inspection of the structure data of two-phase hydride reveals that both lattice parameters (a , b) are reduced by about 2.8–3.1% and we observe the significant expansion in the c direction by about 7.2%. The same effect on the lattice parameters was reported in the hydride synthesized at $p_{\text{H}_2}=2\text{ bar}$ (UFeGeH $_{0.3}$) (Table 2). The unit cell expansion reaches 1.3%, which is probably the upper limit for the α -hydride. Estimated hydrogen content in both phases is 0.3 H/f.u. $_{\text{orth}}$ and 2.0 H/f.u. $_{\text{hex}}$.

In order to avoid the phase coexistence, the highest available hydrogen pressure of 156 bar was applied to synthesize the pure β -hydride of UFeGe. The attempt was successful, yielding the hydride crystallizing in the hexagonal ZrBeSi-type of structure and exhibiting 5.5% volume expansion. The H content was estimated to be between 1.7 and 1.8 H/f.u. The comparison between XRD patterns for pure UFeGe and its hydrides is shown in Fig. 1.

For comparison, the high hydrogen pressure of 140 bar was also applied on UFeSi. The parent compound crystallizes in the TiNiSi-type of structure. The result of hydrogenation is also the two-phase hydride. In this case 70% of the orthorhombic phase was transformed to the hexagonal one (ZrBeSi-type) with a concomitant volume expansion of 13%, the rest remaining as non-expanded orthorhombic phase. We can therefore conclude that no α -hydride can be observed. Apparently, the hydrogen pressure of

140 bar is not sufficient to synthesize a single-phase hydride of UFeSi.

3.2. Magnetic properties

Considering uranium compounds, the U–U spacing (d_{U-U}), is the prominent parameter tuning magnetic properties. For small U–U spacing, below the Hill limit (3.4–3.6 Å), the 5*f*–5*f* wave functions overlap is strong and the 5*f* band becomes broader; such compounds are often found to have a superconducting and non-magnetic ground state. In the case of large d_{U-U} , the 5*f*–5*f* wave functions overlap is weak, the band becomes narrower and 5*f* electrons have a tendency to localization. The ground state is typically

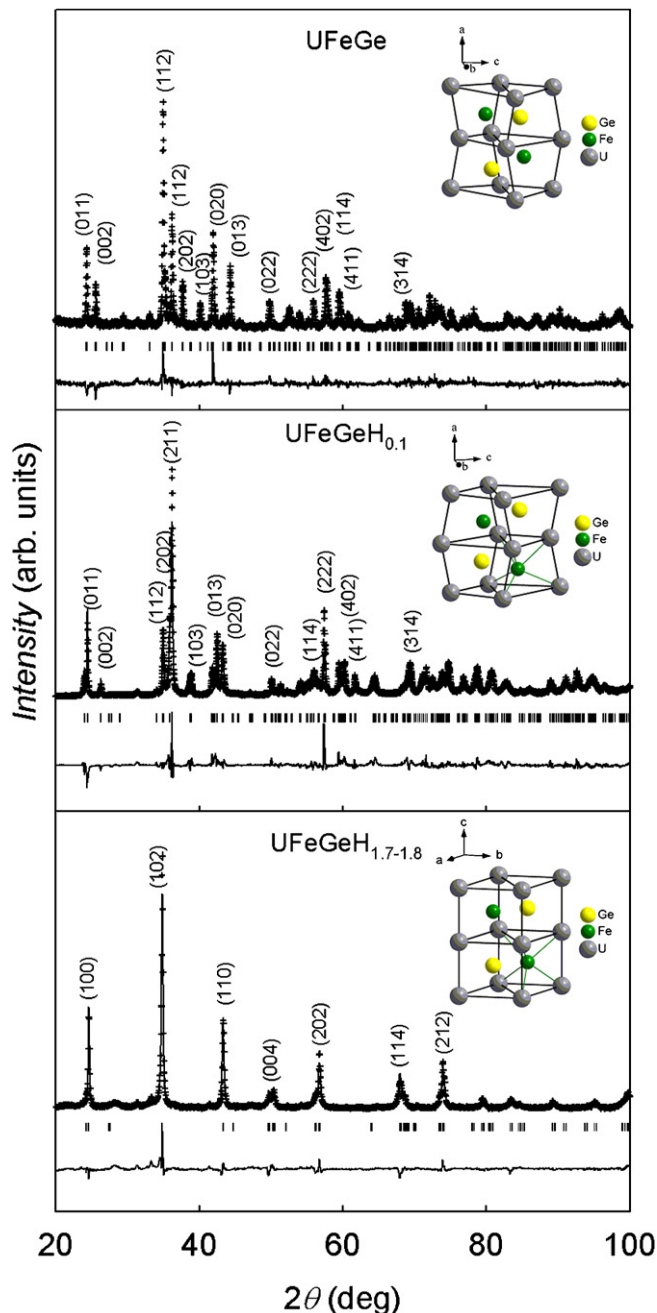


Fig. 1. Rietveld refinement of UFeGe and its hydrides, showing the observed (crosses) and calculated (line) diffraction patterns, reflection tick marks (vertical lines), principal Miller indices, and difference profile (lower line). The insets show the corresponding unit cells.

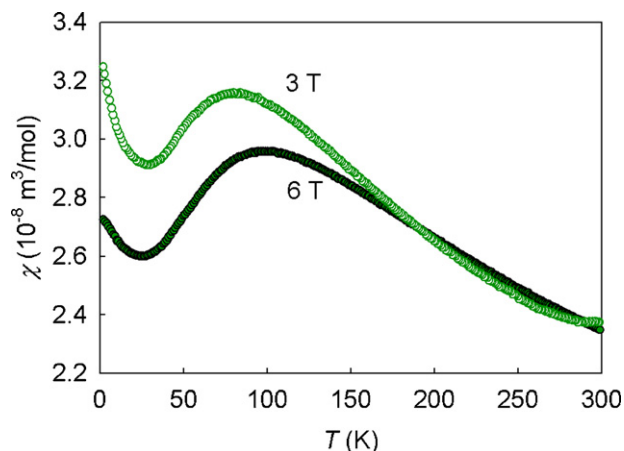


Fig. 2. Temperature dependence of the magnetic susceptibility of UFeGe measured in the magnetic fields $\mu_0 H = 3$ and 6 T.

non-superconducting, often magnetic. One has also to take into consideration the existence of the exceptions from the Hill rule, due to the 5*f*-ligand hybridization, which works as another delocalizing mechanism besides the 5*f*–5*f* overlap. Therefore in this case additional parameters stimulating or suppressing the magnetism have to be considered. The shortest U–U distance in UFeGe-like monoclinic structure can be expressed as

$$d_{U-U} = \sqrt{(x_{U2} - x_{U1})^2 a^2 + (z_{U2} - z_{U1})^2 c^2 - 2ac(x_{U2} - x_{U1})(z_{U2} - z_{U1}) \sin \beta} \quad (1)$$

where x_{U1} , z_{U1} and x_{U2} , z_{U2} are the coordinates of U1 and U2 atoms, respectively, a , c are the lattice parameters and β is the angle between the a and c axes. As it is seen from Eq. (1), it does not depend on the lattice parameter b . The value of the shortest U–U distance is calculated to be 3.45 Å, which is in the boundary range of the Hill limit. The shortest U–Fe and U–Ge distances (<3.00 Å) may suggest an importance of the uranium–ligand hybridization in the delocalization of 5*f* states.

These facts are in an agreement with the experiment [2], proving that the ground state of UFeGe is non-magnetic. In the hexagonal hydride a significant increase of d_{U-U} ($=c/2$) up to 3.67 Å together with an increase of both U–Fe and U–Ge distances up to 3.10 Å was reported. The shortest U–U spacing, which occurs in the case of the orthorhombic structure, i.e. for the α -hydride of UFeGe and pure UFeSi, can be expressed by the formula:

$$d_{U-U} = \sqrt{(0.5a)^2 + [(1.5 - 2z_U)c]^2} \quad (2)$$

where z_U is the coordinate of U atom, a , c are the lattice parameters. From the point of view of U coordination, the U atoms form zig-zag chains along the a_{orth} direction and the distance between the U atoms in-chain is the shortest one. As it is seen in Table 2, d_{U-U} for UFeGeH_{0.3} is unchanged, a reduction of the a lattice parameter is compensated by an expansion in the c direction. An increase of U–ligand spacing (comparable with the β -hydride) may cause the weakening of 5*f*–*d* hybridization and slight tendency towards localization of 5*f* states. In the case of the hexagonal hydride of UFeSi one can observe an opposite effect, here U–Fe and U–Si distances are unchanged, despite an increase of d_{U-U} up to 3.89 Å.

Magnetic susceptibility of the parent UFeGe exhibits the broad maximum around 80 K, in good agreement with [2]. As it is seen in Fig. 2, a small amount of ferromagnetic impurity with $T_C \approx 160$ K is present. It can be probably associated with UFe₂, which has $T_C \approx 160$ –170 K [6]. Also the small hysteresis loop seen in Fig. 3 is a sign of the ferromagnetic impurity, with concentration of the order of 0.1%.

In the case of the UFeGe hydride, the measured susceptibility increases markedly and becomes monotonously increasing with

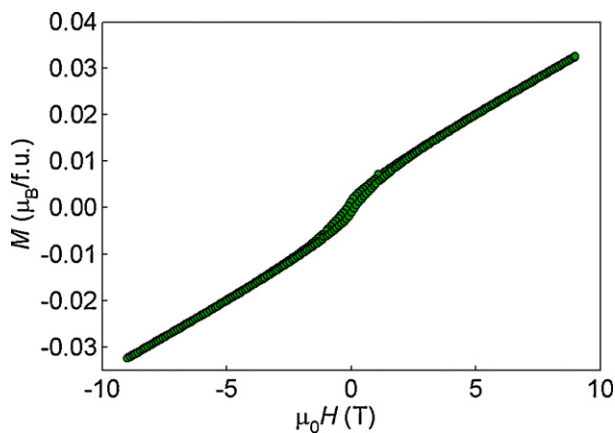


Fig. 3. Hysteresis loop of UFeGe measured at $T = 2$ K.

decreasing T (shown in Fig. 4). The broad maximum seen in UFeGe around 80 K vanishes. Measurements in various magnetic fields (2, 3 and 4 T, not shown here) reveal a certain field dependence, setting up gradually below 300 K, where it is still relatively weak. Although such situation is typical for ferromagnetic impurities, our case does not reveal any particular ordering temperature of the impurity or saturation of the impurity magnetization with decreasing T . The standard procedure for elimination of ferromagnetic impurities (magnetic susceptibility data obtained in two different fields were corrected for a ferromagnetic impurity using the formula: $\chi_{\text{corr}} = (\chi(H_1)H_1 - \chi(H_2)H_2)/(H_1 - H_2)$) yields a very flat $\chi(T)$ on the level of $5 \times 10^{-8} \text{ m}^3 \text{ mol}^{-1}$ followed only by a low temperature upturn (the inset in Fig. 4). More insight can be obtained from the ac susceptibility measurement, which shows only a broad anomaly with maximum between 100 and 150 K for UFeGeH_{1.7–1.8} and between 150 and 200 K for UFeGeH_{0.3} (Fig. 6). This type of measurement is normally selectively sensitive to an onset of ferromagnetism, forming a sharp peak at T_C . Our case indeed indicates a broad distribution of ferromagnetic objects with variable T_C , which can be perhaps understood as due to a distribution of small “ferromagnetic impurity” clusters. We can assume that this impurity can be related to the UFe_{2–x} ($x = 0–0.3$) [6] compound. However, if we calculate the concentration of this kind of impurity, knowing that the spontaneous magnetization of the UFe₂ single crystal is $1 \mu_B/\text{f.u.}$ or less [7], and the remanent magnetization is $0.024 \mu_B/\text{f.u.}$ for UFeGeH_{1.7–1.8} (seen in Fig. 5), we find that the ferromagnetism

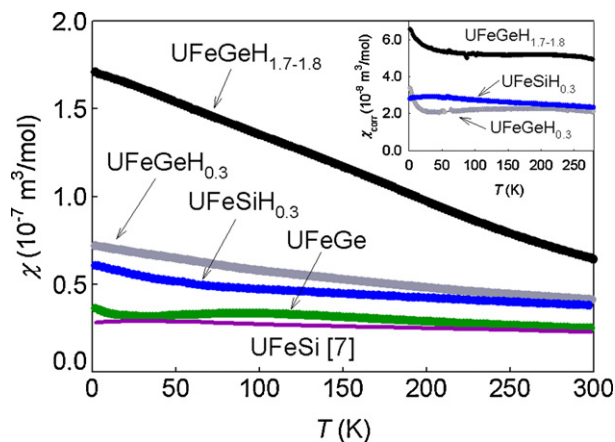


Fig. 4. Temperature dependence of magnetic susceptibility for UFeGe and their hydrides measured in $\mu_0 H = 2$ T. Data of UFeSi were taken from Ref. [7]. The inset shows the temperature dependence of magnetic susceptibility corrected for ferromagnetic impurity at $T = 300$ K.

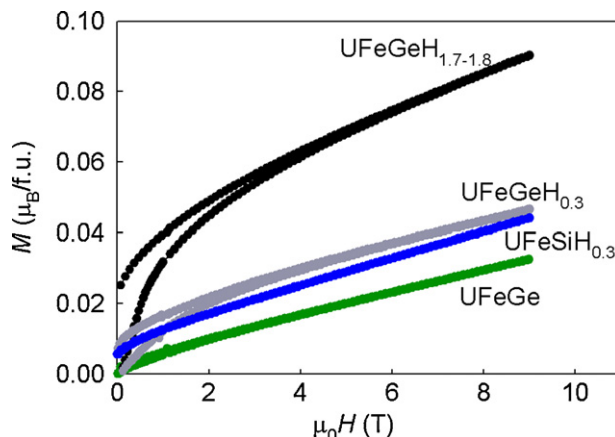


Fig. 5. Magnetization curves of UFeGe, its hydrides and UFeSiH_{0.3} measured at $T = 2$ K.

corresponds only to a small fraction of the sample (2–4%). The magnetization curves of UFeGeH_{1.7–1.8} and UFeGeH_{0.3} measured at 2 K indeed form hysteresis loops with estimated magnetization of $\approx 0.04 \mu_B/\text{f.u.}$ and $0.01 \mu_B/\text{f.u.}$, respectively. The relatively high ordering temperatures (or magnetization-freezing temperatures of the clusters) reaching room temperatures suggest a dominant contribution of the Fe-3d magnetism. The fact that the spontaneous magnetization is not a bulk feature it is further corroborated by ^{57}Fe Mössbauer spectroscopy.

Pure UFeSi similarly to UFeGe shows no signs of magnetic order, however the broad $\chi(T)$ maximum around 80 K observed along the a - and c -axes is reminiscent of spin-fluctuation behaviour [8]. In the case of hydride of UFeSi we observed exactly the same scenario as for UFeGeH_{1.7–1.8}. The measured susceptibility increases (see Fig. 4), the broad maximum seen in UFeSi is not observed in the hydride, $\chi(T)$ measured in various magnetic fields (2, 4 and 8 T) reveals field

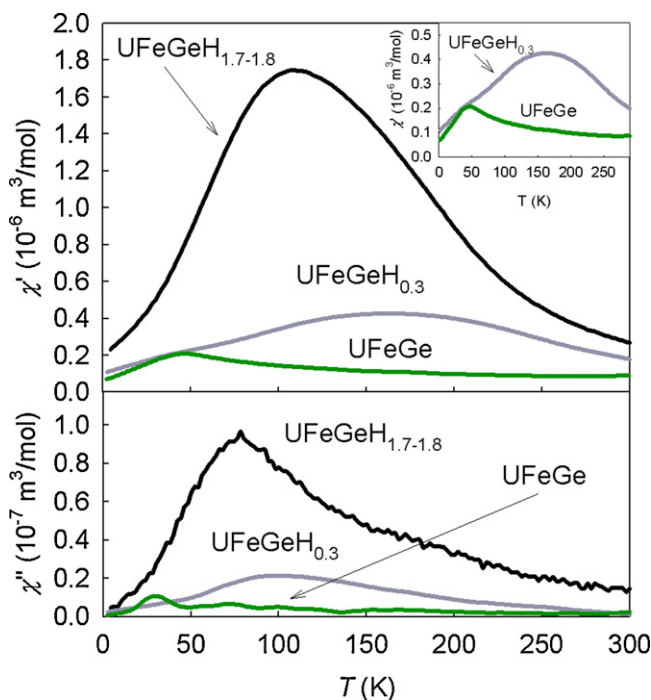


Fig. 6. Temperature dependence of ac susceptibility (real and imaginary part) for UFeGe and its hydrides measured in zero dc field $\mu_0 H = 0$ T, using the frequency 80 Hz.

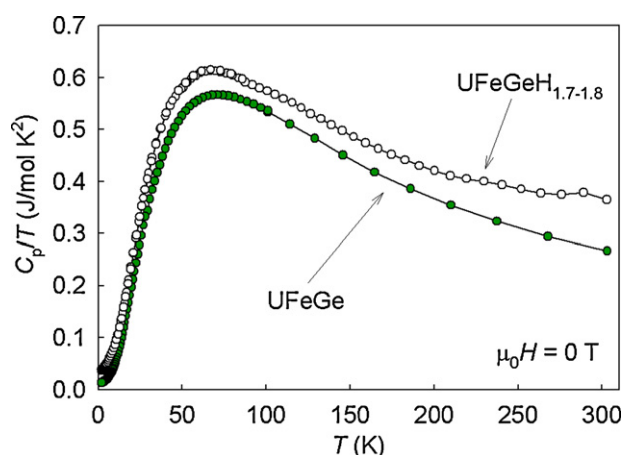


Fig. 7. Temperature dependence of specific heat for UFeGe and its β -hydride.

dependence, pointing to a high temperature ferromagnetic impurity with $T_C > 300$ K.

Specific heat study performed down to $T = 0.4$ K does not indicate any trace of a phase transition in UFeGe or its β -hydride (Fig. 7). In the normal metallic system, the specific heat at low temperatures can be approximated by $C = \gamma T + \beta T^3$. The linear extrapolation of C_p/T vs. T^2 dependence to $T = 0$ K leads to an estimate of the γ coefficient of specific heat about 12 mJ/mol K² for the pure compound. The fitting was done in the T^2 range between 4 and 50 K² (shown by solid lines in Fig. 8). The data above 50 K² deviate from linearity. The values of γ of UTGe compounds (e.g. T = Ni, Pd, Pt) are between 17 and 25 mJ/mol K² [9]. UFeGe has the lowest reported value of γ among the UTGe family. This fact can be understood as due to the strong $5f$ -ligand hybridization leading to the $5f$ -band broadening. The inspection of data in the C_p vs. T representation reveals the Debye temperature $\Theta_D = 270$ K (Fig. 7). Typically the Debye temperature of UTGe compounds is lower than 300 K. The highest reported one is $\Theta_D = 260$ K for UNiGe [10]. In the case of UFeGeH_{1.7-1.8}, the expression of the specific heat adequately fits the data between 4 and 300 K², yielding $\gamma = 36$ mJ/mol K², which indicates a $5f$ -band narrowing. The Debye model does not describe well the $C_p(T)$ for the hydride. It may be due to additional entropy related to vibration modes of H in the lattice and possible H diffusion above $T = 200$ K.

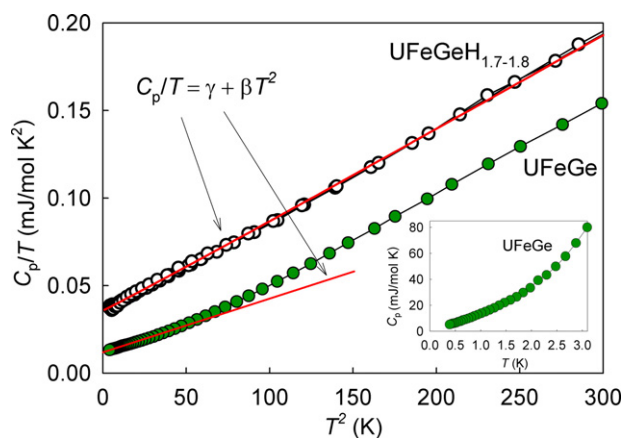


Fig. 8. Temperature dependence of C_p in C_p/T vs. T^2 representation including the linear extrapolation to $T = 0$ K for UFeGe and its β -hydride. The solid lines for the hydride are described in text. The inset shows the ^3He measurement on UFeGe, proving the absence of any phase transition down to 400 mK.

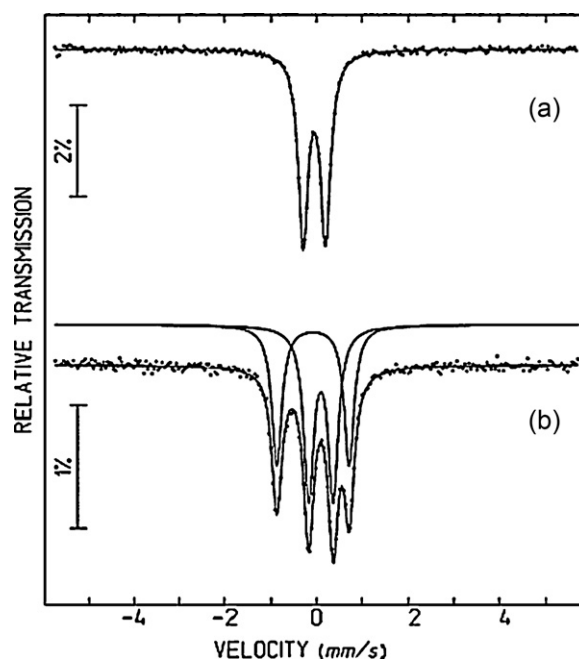


Fig. 9. ^{57}Fe Mössbauer spectra of (a) UFeSi and (b) UFeGe taken at room temperature. The calculated fits are shown by solid lines.

3.3. ^{57}Fe Mössbauer spectroscopy

Mössbauer spectra for UFeGe and its hydride collected at room temperature, $T = 77/80$ K and $T = 4.2$ K are shown in Figs. 9, 11 and 12. Room temperature Mössbauer spectrum of UFeSi was collected for comparison (Fig. 10). Mössbauer spectra were fitted using in the case of UFeGe and its hydride two quadrupole doublets and one quadrupole doublet for UFeSi. The hyperfine parameters extracted from the fit are given in Table 3. In UFeGe as in its hydride there is no magnetic hyperfine field B_{hf} at the Fe atoms even at the temperatures as low as 4.2 K. For UFeGe two different values of isomer shift (IS) and the quadrupole splitting (QS) were reported. The values of relative areas (I) of the iron contribution on each crystallographic site are comparable.

In the UFeGe spectrum the presence of two quadrupole doublets corresponds to the existence of two different crystallographic sites of Fe. It is worth to stress that the value of the QS smaller than 1.00 mm/s is characteristic for a metallic system, however the value

Table 3

Estimated hyperfine parameters from the Mössbauer spectra (isomer shift IS relative to metallic α -Fe, quadrupole splitting QS , line-widths Γ and relative areas I of the Fe contribution on each crystallographic site). Estimated errors for IS , QS , and Γ are ≤ 0.01 mm/s and for $I < 1\%$. Line-width for UFeSi is the total line-width due to the Lorentzian approximation, while for remaining spectra fitted within transmission integral approximation the line-width is the intrinsic absorber line-width.

	Position	T (K)	IS (mm/s)	QS (mm/s)	Γ (mm/s)	I (%)
UFeSi	4c	300	0.08	0.50	0.26	100
		2e-Fe1	0.21	0.53	0.17	54
		2e-Fe2	0.03	1.57	0.16	46
UFeGe	2e-Fe1	77	0.34	0.55	0.20	54
		2e-Fe2	0.16	1.69	0.18	46
	2e-Fe1	4.2	0.34	0.54	0.16	51
		2e-Fe2	0.17	1.70	0.17	49
		300	0.14	0.44	0.27	27
				0.93	0.20	73
UFeGeH _{1.7-1.8}	2c	80	0.26	0.47	0.26	25
			0.97	0.21	0.21	75
		4.2	0.27	0.50	0.28	27
				0.98	0.22	73

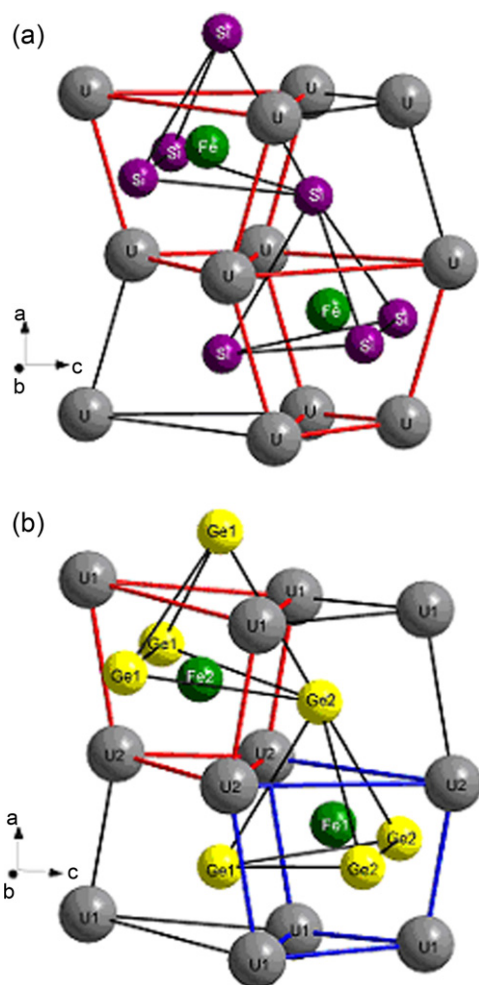


Fig. 10. The unit cell of (a) UFeSi and (b) UFeGe together with the nearest coordination polyhedra.

of the QS greater than 1.00 mm/s is more typical for insulators. As it is seen from Table 3 in the case of UFeGe, the QS value higher than 1.5 mm/s is exceedingly high as the system is found to be metallic [1,2]. Fig. 10 shows the unit cells of both compounds together with the nearest coordination polyhedra of Fe atom. The nearest atomic environment of Fe atoms in 4c position (TiNiSi type of structure) can be considered as a tetrahedron consisting of four silicon atoms (Fig. 10(a)). In the case of UFeGe, the iron atoms occupy 2e position. However the atomic environment of Fe1 and Fe2 is slightly different (Fig. 10(b)). Most likely the weaker QS appears on Fe1 site, as the iron atom is placed in more symmetric environment (inside the tetrahedron consisting of three Ge2 atoms and one Ge1 atom) similarly to the iron atom in UFeSi. This assumption is supported by comparable values of the QS on 2e-Fe1 site and 4c site in UFeSi. The Fe2 atom although surrounded by germanium atoms is not located inside the tetrahedron as in the case of Fe1 and Fe in UFeSi, but a bit below its plane. The second coordination polyhedron is a distorted trigonal prism consisting of three U1 and three U2 atoms.

Since the Fe atom in the hexagonal (ZrBeSi-type) structure occupies single crystallographic (2c) site, one would expect that the Mössbauer spectra at different temperatures consist of a single contribution. Two quadrupole doublets are however necessary to fit the spectra (Fig. 12 and Table 3). Both doublets have similar *IS*. Presence of H atoms in the vicinity of Fe seems not to influence *IS*, so the Fe–H interaction must be weak. The differences of the observed *IS* between the monoclinic UFeGe and the hexagonal UFeGeH_{1.7–1.8} are most probably only due to structural effects. In the hydride all

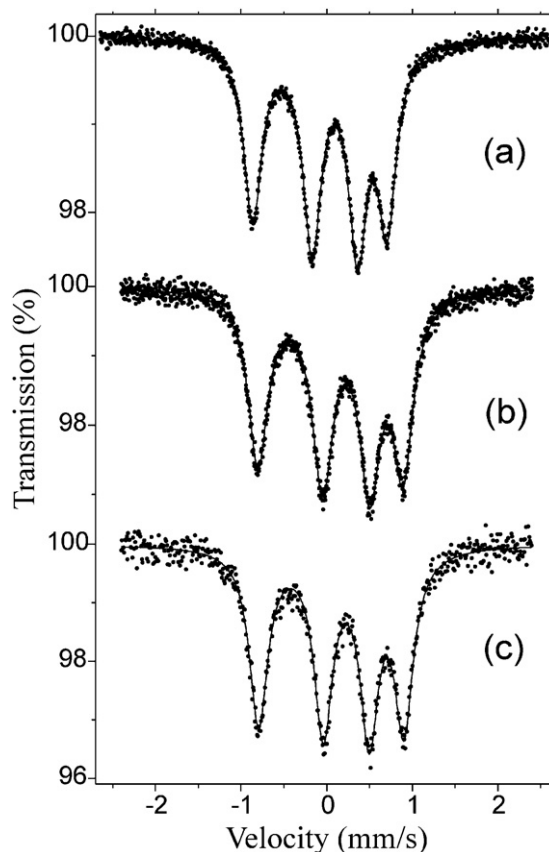


Fig. 11. ⁵⁷Fe Mössbauer spectra of UFeGe taken at (a) 300 K, (b) 77 K and (c) 4.2 K. The calculated fits are shown by solid line.

Fe atoms are lying in the proximity of Ge atoms (2.40 Å), they are not placed inside Ge-tetrahedra, but a bit below one of their faces. The second coordination polyhedron is a trigonal prism consisting of U atoms with Fe located in the middle ($d_{\text{U-Fe}} \approx 3.00$ Å). Two different values of QS are observed in the hydride (Table 3), which can be attributed to different hydrogen coordination numbers of the Fe atoms on the same crystallographic site. In the rare-earth ternary compound LaNiSnD₂ with a similar structural transformation upon hydrogenation [11,12], only one type of D/H positions, surrounded by La₃T in tetrahedral co-ordination, was observed by neutron diffraction. This means that the deuterium atoms in the ZrBeSi-type of structure occupy the 4f (1/3, 2/3, z) sites. The theoretical maximum occupation of each trigonal prism with rare-earth (R) atoms in the corners and transition metal (T) atoms in the centre (forming two R₃T tetrahedra sharing the vertex–T atom) leads to 2 H/f.u. The shortest interatomic distance between deuterium atoms is then $d_{\text{D-D}} \approx 2.78$ Å. Similar position of the deuterium atoms inside the U₃Co tetrahedra was reported for hydrogenated/deuterated uranium ternary compounds, e.g. UCoSnD_{0.6} with the ZrNiAl-type of structure (4h (1/3, 2/3, z) site) [13]. Assuming a similar location of H atoms in the present UFeGeH_{1.7} compound, we can calculate the probability of finding one, two or zero H atoms inside the U₆Fe trigonal prisms. Considering a random distribution of H atoms, the binominal distribution model can be applied:

$$P_n(m) = \frac{n!}{m!(n-m)!} y^m (1-y)^{n-m} \quad (3)$$

where $n=2$, is the maximum number of nearest H-neighbours of Fe atoms, $P_n(m)$ with $m=0$ or 1 or 2, is the probability of finding m nearest H-neighbours of Fe atoms, and finally y is the fraction of the possible sites occupied by H atoms ($y=1.7/2=0.85$ for UFeGeH_{1.7}).

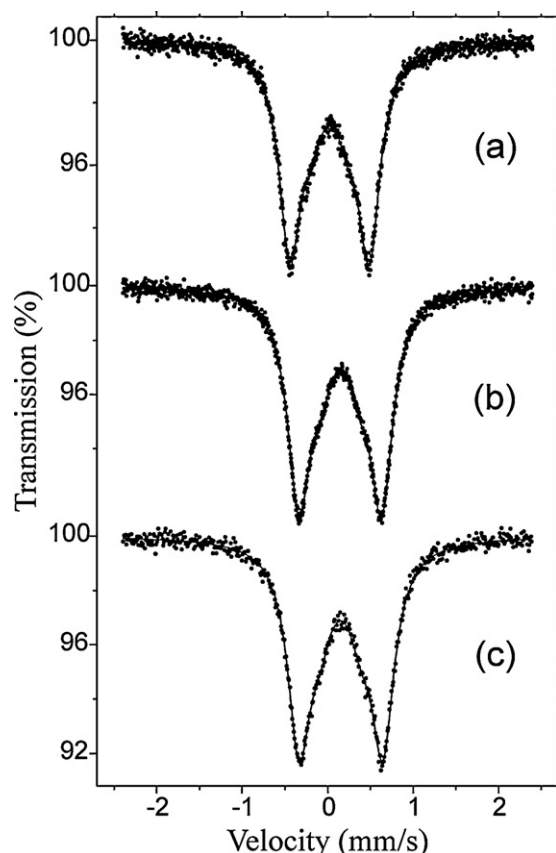


Fig. 12. ^{57}Fe Mössbauer spectra of $\text{UFeGeH}_{1.7-1.8}$ taken at (a) 300 K, (b) 80 K and (c) 4.2 K. The calculated fits are shown by solid line.

The probability of finding two nearest H-neighbours of Fe atom is 0.72 and the probability of finding one nearest H-neighbour is 0.25, which is in good agreement with the relative areas I of the Fe contributions estimated for each quadrupole doublet in the spectra of the hydride with H concentration of 1.7 H/f.u.

A long-range magnetic order of the Fe sublattice at low temperatures is definitely excluded by ^{57}Fe Mössbauer spectroscopy, for both UFeGe and its hydride. The increase of the IS with decreasing temperature is that usually observed in Fe systems due to the second order Doppler effect [14].

4. Discussion and conclusions

In the present paper, we have reported the effect of hydrogenation on the magnetic properties of UFeGe . The $5f$ states in the pure UFeGe are strongly affected by the $5f$ - d hybridization, which is responsible for the non-magnetic ground state. As the short-

est distance between the U2–Fe2 atoms ($\approx 2.35 \text{ \AA}$) is very small in comparison to e.g. UFe_2 with $d_{\text{U-Fe}} \approx 2.93 \text{ \AA}$. As given by electronic structure calculations [2], the strong hybridization is then responsible for the suppression of the magnetism. The $d_{\text{U-U}}$ is just at the boundary of the Hill limit.

The hydrogenation of a paramagnetic UFeGe changes the type of crystal structure from the UFeGe -like monoclinic to the orthorhombic (TiNiSi-type) or the hexagonal (ZrBeSi-type) one. The increase of $d_{\text{U-U}}$ (up to 3.67 \AA) and other types of interatomic spacings are not sufficient to induce a real magnetic order, only the susceptibility increase. This fact was confirmed by the low-temperature Mössbauer experiment for β -hydride of UFeGe , which showed no stable moments within the Fe sublattice. Although Fe occupies only one crystallographic site in the β -hydride two different values of the QS were observed due to different H coordination. The probability of finding two H atoms as the nearest neighbours of Fe atom is three times larger than in the case of one H occupying U_6Fe trigonal prism. The magnetic clusters with probable Fe magnetism dominance can be observed in the hydrides. A possible subject of further research would be the electronic structure calculations for the hydride phases of UFeGe .

Acknowledgements

This work was part of the research program MSM 0021620834 and by the Czech-Portuguese exchange program GRICES/ASCR 2009. A.M.A. was partly supported by the Grant Agency of the Czech Republic under the grant No. 202/09/11N9.

References

- [1] F. Canepa, P. Manfrinetti, M. Pani, A. Palenzona, J. Alloys Compd. 234 (1996) 225.
- [2] L. Havela, A. Kolomiets, V. Sechovsky, M. Diviš, M. Richter, A.V. Andreev, J. Magn. Mater. 177–181 (1998) 47.
- [3] A.M. Adamska, A.V. Kolomiets, J. Pospíšil, L. Havela, J. Phys.: Conf. Ser. 200 (2010) 012002.
- [4] A.M. Adamska, A.V. Kolomiets, J. Pospíšil, L. Havela, IOP Conf. Ser.: Mater. Sci. Eng. 9 (2010) 012051.
- [5] A. Adamska, L. Havela, K. Eichinger, J. Pospíšil, K. Miliyanchuk, Int. J. Mater. Res. 100 (2009) 1230–1233.
- [6] A.T. Aldred, J. Magn. Mater. 10 (1979) 42.
- [7] A.V. Andreev, D.A. Filippov, R.Z. Levitin, V.V. Snegirev, J. Magn. Mater. 258–259 (2003) 555–557.
- [8] A.V. Andreev, F. Honda, V. Sechovsky, M. Diviš, N. Izmaylov, O. Chernyavski, Y. Homma, Y. Shiokawa, J. Alloys Compd. 335 (2002) 91–94.
- [9] S. Kawamata, H. Iwasaki, N. Kobayashi, J. Magn. Mater. 104–107 (1992) 55–56.
- [10] I.H. Hagmusa, J.C.P. Klaasse, E. Bruck, K. Prokes, F.R. de Boer, H. Nakotte, J. Appl. Phys. 81 (1997) 4157–4159.
- [11] H.W. Brinks, V.A. Yartys, B.C. Hauback, J. Alloys Compd. 322 (2001) 160.
- [12] V.A. Yartys, T. Olavesen, B.C. Hauback, H. Fjellvåg, H.W. Brinks, J. Alloys Compd. 330–332 (2002) 141–145.
- [13] K. Miliyanchuk, L. Havela, J.C. Waerenborgh, P. Gaczyński, O. Prokhnenko, Chem. Met. Alloys 1 (2008) 174–179.
- [14] N.N. Greenwood, T.C. Gibb (Eds.), Mössbauer Spectroscopy, Chapman Hall Ltd., London, 1971.